

# 1/f noise in magnetic tunnel junctions with MgO tunnel barriers

Aisha Gokce<sup>a)</sup> and E. R. Nowak

Department of Physics and Astronomy, University of Delaware, Newark, Delaware 19716

See Hun Yang and S. S. P. Parkin

IBM Almaden Research Center, San Jose, California 95120

(Presented on 31 October 2005; published online 27 April 2006)

Electrical noise measurements are reported for magnetic tunnel junctions having magnesium oxide tunnel barriers. These junctions have resistance-area products (RAPs) of order 10–100 M $\Omega$   $\mu\text{m}^2$  and exhibit zero-bias tunneling magnetoresistance ratios (TMRs) as high as 120% at room temperature. The TMR is bias dependent and decreases to half its maximum value for biases near 300 mV. The dominant low-frequency electrical noise is due to resistance fluctuations having a 1/f-like power spectral dependence and a nonmagnetic origin. The normalized 1/f noise parameter,  $\alpha$ , is found to be of order  $10^{-7}$  to  $10^{-6}$  which compares favorably to magnetic tunnel junctions consisting of an aluminum oxide barrier with comparable RAPs but lower TMR. At high biases,  $\alpha$  is found to decrease which we attribute to defect-assisted tunneling mechanisms. © 2006 American Institute of Physics. [DOI: 10.1063/1.2169591]

The development and advances of spin-dependent tunneling structures for memory<sup>1,2</sup> and sensor<sup>3,4</sup> applications have largely focused on using amorphous aluminum oxide tunnel barriers. Magnetic tunnel junctions (MTJs) consisting of CoFeB magnetic electrodes and AlO<sub>x</sub> barriers have attained tunneling magnetoresistance ratio (TMR) up to ~70% at room temperature and low fields. Recent reports<sup>5,6</sup> of TMR >220% have renewed interest in using polycrystalline and epitaxial tunnel barriers, particularly magnesium oxide. MTJs made using MgO tunnel barriers show a threefold increase in output voltage compared to AlO<sub>x</sub> barriers. For magnetic-field sensor applications, both signal and noise determine the minimum detectable magnetic field. Indeed, 1/f noise is a performance limiting factor in MTJs at low frequencies ( $f < 100$  Hz).<sup>7,8</sup> Here, we report low-frequency noise studies of MgO-based MTJs and draw comparisons to AlO<sub>x</sub>-based MTJs.

The MTJs used in these studies were fabricated similarly to those reported in Ref. 5 and were patterned by *in situ* shadow masks to give cross-shaped geometries with junction areas of 80 × 80 or 80 × 300  $\mu\text{m}^2$ . Our most extensive studies are on MTJs having the following materials, stack: Si(100)/SiO<sub>2</sub>/TaN/Ta/IrMn/CoFe/MgO/CoFe/CoFeB/TaN/Pt. The CoFeB layer gives rise to improved magnetics and higher thermal stability. The latter is needed because the highest TMR values are found for the highest possible annealing temperatures (>420 °C). The MTJs we investigated were annealed at 300 °C but not optimized to yield the highest TMR.

A typical magnetoresistance curve is shown in Fig. 1. The field range is sufficiently large that both the switching of the exchange-biased lower ferromagnetic electrode and the upper ferromagnetic electrode are seen. The magnetics of the materials' stack is designed to yield a hysteretic response at zero field that is suitable for memory applications rather than

a linear response which is desirable for sensors. TMR values of ~120% at room temperature were found. The TMR was also found to decrease with bias voltage (see Fig. 1 inset), dropping to half at a voltage of ~0.3 V, symmetrically for both positive and negative voltages. The barrier height of the MgO tunnel barrier was estimated from current versus voltage ( $I$ - $V$ ) curves<sup>9</sup> to be ~0.9 eV at both 10 and 300 K. The small barrier height suggests that MgO barriers contain oxygen defect states that form an impurity band inside the energy gap of MgO.<sup>6</sup>

Conventional four-probe noise measurements were performed using constant current bias. The power spectral density of the voltage fluctuations followed a nominally 1/f dependence at low frequencies crossing over to a frequency-independent (white) behavior above ~1–10 kHz. The magnitude of the white noise was consistent with the Johnson-shot noise relation.<sup>10</sup> The 1/f noise characteristics are conveniently parametrized by the quantity  $\alpha$  which is defined<sup>10</sup> as  $\alpha \equiv fAS_V/I^2R^2$ , where  $A$  is the junction area,  $S_V$  is the measured power spectral density, and the other terms have their usual meaning.  $\alpha$  can be used to compare the noise from different sized MTJs measured under different

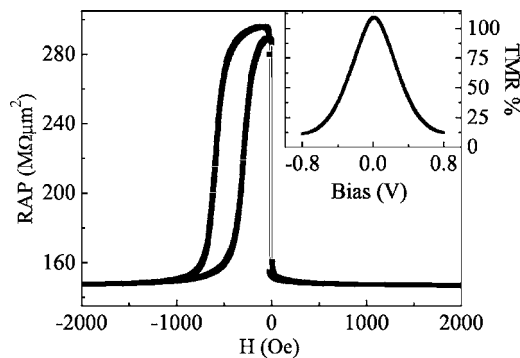


FIG. 1. RAP vs magnetic field measured at 300 K and  $I=20$   $\mu\text{A}$ . Inset: voltage bias dependence of the TMR calculated using  $(R_{AP}-R_P)/R_P$ .

<sup>a)</sup>Electronic mail: cgokce@udel.edu

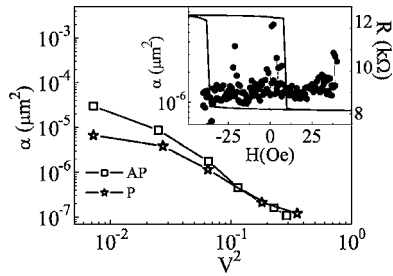


FIG. 2. Bias dependence of the noise magnitude at 300 K. The rectangles represent the noise measured in the AP configuration and the stars represent the  $P$  configuration. Inset: noise as a function of field taken at  $I=20 \mu\text{A}$ . The magnetoresistance is denoted by the solid line.

bias conditions, provided that  $S_V$  scales as  $1/f$  and as the square of the current or voltage bias, as expected for resistance fluctuations. However, the parameter  $\alpha$  was found to decrease with bias, as shown in Fig. 2. The decrease is significant at high bias and appears to correspond to the onset of strong nonlinearity in the  $I$ - $V$  curves. This behavior is discussed further below. In the remainder of the paper we continue to describe the  $1/f$  noise in terms of  $\alpha$  with the understanding that it is bias dependent.

We have also studied the magnetic field dependence of the  $1/f$  noise at small fields. The inset to Fig. 2 shows that  $\alpha$  is essentially independent of field except at a few fields that show narrow spikes in noise power. At these fields, deviations from a  $1/f$  spectrum are found and in some cases can be associated with random telegraph noise in the time domain. Some of the spikes occur near fields at which the free layer is undergoing a reversal of its magnetization direction. In previous work on  $\text{AlO}_x$ -based MTJs,<sup>7</sup> we were able to correlate such spikes in noise with metastability in the magnetization of the free layer. A plausible explanation based on small barrier height, bias dependence of random telegraph noise at magnetically stable configurations, and bias dependence of  $\alpha$  is that the noise has nonmagnetic origins, e.g., charge traps in or near the tunnel barrier.

The temperature dependence of the  $1/f$  noise is shown in Fig. 3. For these data, a 100 Oe field was applied to maintain a parallel ( $P$ ) configuration of the magnetizations in the electrodes so that the  $1/f$  noise was due to electronic rather than magnetic origins.  $\alpha$  is seen to decrease rapidly below room temperature and tends to level out at temperatures below  $T \sim 160$  K. At low  $T$ ,  $\alpha$  is a factor of 500 less than at 300 K. The drop in noise power with decreasing temperature is sharper than what was observed in MTJs hav-

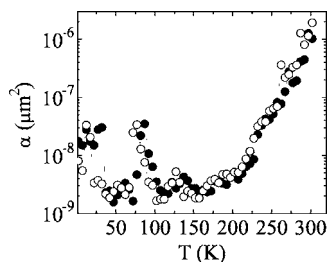


FIG. 3. Plotted is the temperature dependence of  $\alpha$ . The solid (open) symbols denote the data taken upon increasing (decreasing) temperature in  $P$  configuration using  $I=34 \mu\text{A}$ .

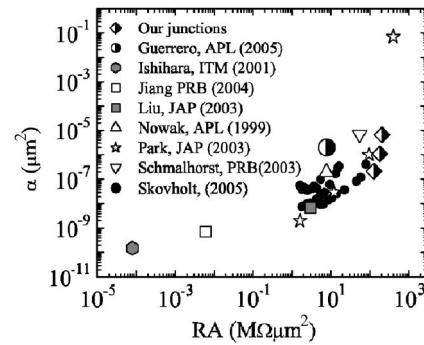


FIG. 4. Compilation plot of the nonmagnetic noise as a function of RAP for MTJs from various sources. The semisolid diamonds and circle denote MgO-based MTJs; all other symbols are for  $\text{AlO}_x$  barriers.

ing  $\text{AlO}_x$  barriers.<sup>7</sup> We note that the temperature dependence is largely reproducible upon warming up and cooling down—the slight shift in the curves is likely due to the sample stage not being in thermal equilibrium. The spikes in  $\alpha$  around 80 and 25 K are due to a large random telegraph signal. The kinetics of the fluctuating entity showed a strong temperature dependence across our measurement bandwidth. The predominant effect of increasing  $T$  was to shorten the lifetimes of each resistance state with a little change in duty cycle.

Figure 4 plots the magnitude of the electronic  $1/f$  noise as a function of resistance-area product (RAP). Data are compiled for different tunnel junctions from a number of sources.<sup>7,10–16</sup> In the majority of cases, the tunnel barrier was  $\text{AlO}_x$ . It is observed that  $\alpha$  increases with RAP, particularly above  $\text{RAP} \sim 1 \text{ M}\Omega \mu\text{m}^2$ . Higher noise levels may be expected if defect-assisted tunneling occurs in thicker oxide barriers. Interestingly, the electronic noise level at low RAP seems to have reached a lower bound of  $\sim 10^{-10} \mu\text{m}^2$  for aluminum oxide barriers. The semisolid diamond symbols denote our MgO-based MTJs and the semisolid circle symbol is for the Fe/MgO(111)/Fe epitaxial MTJs from Guerrero *et al.*<sup>11</sup> Because  $\alpha$  is a function of bias in our MTJs, there is a corresponding spread in data in Fig. 4. MgO-based MTJs having a (100)-oriented tunnel barrier appear to be somewhat less noisy than  $\text{AlO}_x$  MTJs at a comparable RAP.

Finally, we discuss the influence of defect states in the MgO tunnel barrier on  $I$ - $V$  curves and noise. The low barrier heights we deduce by fitting the  $I$ - $V$  curves to Simmons' model<sup>9</sup> are in agreement with other reports<sup>5,17,18</sup> and attributed to oxygen vacancies positioned  $\sim 1$ – $2$  eV below the conduction band in MgO. If oxygen or other defect states exist in the barrier then the electron tunneling process may involve “hopping” through one or more localized states, particularly for thicker barriers. In the theory put forth by Xu *et al.*,<sup>19</sup> the combination of direct and inelastic tunnelings through localized states leads to a voltage dependence of the tunneling conductance given by

$$\sigma(V) = \sigma_o + \sigma_1 + \sigma_2 V^{n_2} + \dots + \sigma_x V^{n_x}, \quad (1)$$

where  $\sigma$  is the junction conductance,  $\sigma_o$  is the direct tunneling conductance,  $\sigma_x$  is the conductance for an electron hopping  $x$  number of times through the barrier, and  $n_x$  is the corresponding exponent. Both direct tunneling and resonant

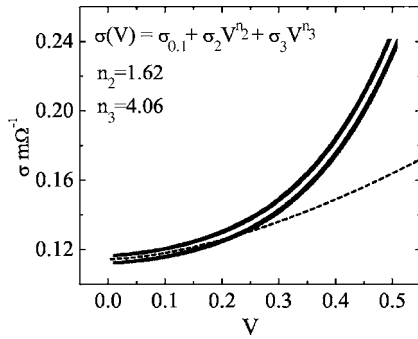


FIG. 5. The solid line shows the bias dependence of the conductance in the  $P$  configuration at 300 K. The dashed line is a fit to Eq. (1) for defect-assisted tunneling including terms up to  $x=2$ . The  $x=3$  term is included in the fit denoted by the white line.

tunneling ( $x=1$ ) are independent of bias, while higher-order ( $x \geq 2$ ) defect-assisted tunneling mechanisms are bias dependent. At low-voltage biases (a few times  $k_B T$ ), the electron tunneling is expected to be predominately from direct tunneling and defect-assisted tunneling with up to two hops ( $x=2$ ) through the barrier with a predicted exponent  $n_2=4/3$ . Three-step hopping results in  $n_3=5/2$ .

Figure 5 shows the fitting of Eq. (1) to tunneling conductance data taken at 300 K in the  $P$  configuration. Prominent zero-bias conductance anomalies precluded an analysis of low-temperature ( $<100$  K) data. The fitting was done in two stages, as described in Ref. 19. First, low bias ( $V < 100$  mV) data were used to determine the values of the first three parameters in Eq. (1). The fit yielded  $\sigma_0 + \sigma_1 = 0.115 \text{ m}\Omega^{-1}$ ,  $\sigma_2 = 0.152 \text{ m}\Omega^{-1}$ , and  $n_2 = 1.62$ . It is denoted by the dashed line in Fig. 5 where it has been extrapolated to higher bias voltages for clarity. We also found that the value of  $n_2$  is not sensitive to the range chosen for the fit when restricted to below 100 mV. Keeping  $\sigma_0 + \sigma_1$ ,  $\sigma_2$ , and  $n_2$  fixed at the values listed above, and allowing  $\sigma_3$  and  $n_3$  to vary as free parameters, we fit the conductance data from 0 to 500 mV and found the best fit for  $n_3$  as 4.06. The solid white line in Fig. 5 shows the best fit with the addition of the  $x=3$  term.

The fit is very good although the exponents, especially  $n_3$ , differ from theory. The discrepancy may be due to the need to include higher-order processes in the case of high-temperature data. Also, some of the bias dependence may be the result of rapidly varying density of states in the magnetic electrodes near the Fermi level.

Although inelastic hopping through localized states in the barrier may not fully account for the  $\sigma(V)$  data, localized states are also a plausible explanation for some of the unusual noise data we observe, such as the bias-dependent tele-

graph noise and the decrease in  $\alpha$  with increasing  $V$ . For instance, as the bias voltage increases, hopping chains with more than one localized state may result in high-conductance, low noise channels which would cause  $\alpha$  to decrease. Interestingly,  $\alpha$  begins to decrease rapidly above  $\sim 200$  mV which corresponds to the onset of strong nonlinearity in the  $I$ - $V$  curves. The extent to which on-site Coulomb interactions between electrons during the hopping process is responsible for the random telegraph noise and the low-temperature zero-bias conductance anomalies needs to be clarified.

In comparison to  $\text{AlO}_x$  barriers,  $\text{MgO}$  barriers offer a threefold increase in TMR without an additional low-frequency noise. (Note that we have examined a comparatively small number of  $\text{MgO}$ -based MTJs, hence our statistics are poor.) These characteristics are favorable for advancing both sensor and memory technologies. A further improvement in low-frequency performance is anticipated as the materials' stack becomes optimized not only for TMR signal but also for noise properties.

The work at Delaware was supported in part by the National Science Foundation through Award No. 0405136, the donors of The American Chemical Society Petroleum Research Fund, and through the Cottrell Scholar Program of the Research Corporation.

<sup>1</sup>S. S. P. Parkin, Proc. IEEE **91**, 661 (2003).

<sup>2</sup>S. Tehrani, B. Engel, J. M. Slaughter *et al.*, IEEE Trans. Magn. **36**, 2752 (2000).

<sup>3</sup>M. Tondra, J. M. Daughton, C. Nordman *et al.*, J. Appl. Phys. **87**, 4679 (2000).

<sup>4</sup>M. Tondra, J. M. Daughton, D. Wang *et al.*, J. Appl. Phys. **83**, 6688 (1998).

<sup>5</sup>S. S. P. Parkin, C. Kaiser, A. Panchula *et al.*, Nat. Mater. **3**, 862 (2004).

<sup>6</sup>S. Yuasa, T. Nagahama, A. Fukushima *et al.*, Nat. Mater. **3**, 868 (2004).

<sup>7</sup>L. Jiang, E. R. Nowak, P. E. Scott *et al.*, Phys. Rev. B **69**, 054407 (2004).

<sup>8</sup>N. A. Stutzke, S. E. Russek, and D. P. Pappas, J. Appl. Phys. **97**, 10Q107 (2005).

<sup>9</sup>J. G. Simmons, J. Appl. Phys. **34**, 1793 (1963).

<sup>10</sup>E. R. Nowak, M. B. Weissman, and S. S. P. Parkin, Appl. Phys. Lett. **74**, 600 (1999).

<sup>11</sup>R. Guerrero, F. G. Aliev, R. Villar *et al.*, Appl. Phys. Lett. **87**, 042501 (2005).

<sup>12</sup>K. Ishihara, M. Nakada, E. Fukami *et al.*, IEEE Trans. Magn. **37**, 1687 (2001).

<sup>13</sup>X. Liu and G. Xiao, J. Appl. Phys. **94**, 6218 (2003).

<sup>14</sup>W. K. Park, J. S. Moodera, J. Taylor *et al.*, J. Appl. Phys. **93**, 7020 (2003).

<sup>15</sup>J. Schmalhorst and G. Reiss, Phys. Rev. B **68**, 224437 (2003).

<sup>16</sup>J. F. Skovholt, L. Jiang, E. R. Nowak *et al.*, (unpublished).

<sup>17</sup>T. Kiyomura, Y. Maruo, and M. Gomi, J. Appl. Phys. **88**, 4768 (2000).

<sup>18</sup>S. Mitani, T. Moriyama, and K. Takanashi, J. Appl. Phys. **93**, 8041 (2003).

<sup>19</sup>Y. Xu, D. Ephron, and M. R. Beasley, Phys. Rev. B **52**, 2843 (1995).